Published in final edited form as:

Environ Microbiol. 2018 November ; 20(11): 4184–4193. doi:10.1111/1462-2920.14431.

Diatom populations in an upwelling environment decrease silica content to avoid growth limitation

Heather M. McNair[*,a,b], **Mark A. Brzezinski**[a,c], and **Jeffrey W. Krause**[d,e]

[a.]Department of Ecology, Evolution and Marine Biology, University of California Santa Barbara, Santa Barbara, CA, 93106

[b.]Current address: Graduate School of Oceanography, University of Rhode Island, Narragansett, RI 02882

[c.]Marine Science Institute, University of California Santa Barbara, Santa Barbara, CA, 93106

[d.]Dauphin Island Sea Lab, University of South Alabama, Dauphin Island, AL, 36528

[e.]Department of Marine Sciences, University of South Alabama, Mobile, AL 36688

Summary

A mix of adaptive strategies enable diatoms to sustain rapid growth in dynamic ocean regions, making diatoms one of the most productive primary producers in the world. We illustrate one such strategy off coastal California that facilitates continued, high, cell division rates despite silicic acid stress. Using a fluorescent dye to measure single-cell diatom silica production rates, silicification (silica per unit area) and growth rates we show diatoms decrease silicification and maintain growth rate when silicon concentration limits silica production rates. While this physiological response to silicon stress was similar across taxa, *in situ* silicic acid concentration limited silica production rates by varying degrees for taxa within the same community. Despite this variability among taxa, silicon stress did not alter the contribution of specific taxa to total community silica production or to community composition. Maintenance of division rate at the expense of frustule thickness decreases cell density which could affect regional biogeochemical cycles. The reduction in frustule silicification also creates an ecological tradeoff: thinner frustules increase susceptibility to predation but reducing Si quotas maximizes cell abundance for a given pulse of silicic acid, thereby favoring a larger eventual population size which facilitates diatom persistence in habitats with pulsed resource supplies.

Introduction

Diatoms, silicified unicellular phytoplankton, are among the most ecologically diverse and successful organisms in the ocean (Kooistra *et al*., 2007; Malviya *et al*., 2016), generating ~40% of global marine primary production (Nelson *et al*., 1995). Diatoms thrive in dynamic ocean environments (Nelson *et al*., 1995) where physical mixing brings pulses of nutrients to the sunlit-surface ocean. In these regions, diatoms create dense blooms using a complex mix

[*]Corresponding author: hmcnair@uri.edu.

The authors declare no conflict of interest.

of r-selected strategies—which prioritize rapid and sustained cell division. This is contrasted by organisms that use K-selected strategies which prioritize persistence in environments near carrying capacity, e.g. dinoflagellates (Margalef, 1978). Among the r-selected strategies employed by diatoms are thought to be physiological adjustments for maintaining growth with rapidly decreasing nutrient availability (e.g. Guillard *et al.*, 1973; Paasche, 1975).

The capacity of phytoplankton cells to maintain division rates as resources are depleted influences not only succession among classes of phytoplankton (Egge and Aksnes, 1992) but also succession within a class due to interspecies differences in nutrient use (Tilman, 1977; Kilham and Tilman, 1979). Diatoms are unique among phytoplankton in their obligate requirement for silicic acid, $Si(OH)_4$, which is an essential component of the diatom siliceous cell wall or frustule. In all ocean provinces examined to date, including highly productive coastal (Nelson and Dortch, 1996) and polar regions (Nelson and Tréguer, 1992; Nelson *et al.*, 2001), silicic acid concentration, $[Si(OH)_4]$, episodically or chronically limits diatom silica production rates (hereafter referred to as 'silicon stress'). The unique requirement of silicon and the pervasiveness of silicon stress has led to the conclusion that $[Si(OH)_4]$ contributes to phytoplankton succession (Egge and Aksnes, 1992; Lochte *et al.*, 1993; Sieracki *et al.*, 1993; Merico *et al.*, 2004). However, culture experiments have found that diatoms are capable of decoupling silica production rates and cell division rates when $Si(OH)_4$ becomes scarce—implying that cells decrease their silicon requirement to delay the onset of growth limitation (Guillard *et al.*, 1973; Paasche, 1973a; Brzezinski *et al.*, 1990).

The physiological progression of diatoms first reducing frustule silica content and then decreasing division rate was described in culture experiments 45 years ago (Paasche, 1973a). The decoupled decrease in rates of silicon uptake (determined by net drawdown of $Si(OH)_4$) and division (determined from cell abundance) implied a decrease in silicification and frustule thinning. Subsequent laboratory studies documented the same hierarchical response to silicon stress in a number of species (Martin-Jézéquel *et al.*, 2000 and references therein) suggesting decreasing silicification could be a common strategy for avoiding silicon growth limitation in the ocean. Cultured strains were shown to decrease their frustule silicon content three- to four-fold under severe silicon stress without significant decreases in growth rate (Guillard *et al.*, 1973; Paasche, 1975; Brzezinski *et al.*, 1990). This implies that in natural diatom populations $[Si(OH)_4]$ would need to limit silica production rates to 25–33% of maximum before division rates would slow significantly. Given that diatom silica production follows Michaelis-Menten kinetics (Sup. Info.) with a median half-saturation constant of ~2 μM $Si(OH)_4$ (Martin-Jézéquel *et al.*, 2000), the plasticity in silica content facilitates near maximum division rates until $Si(OH)_4$ decreases below 1 μM. Directly assessing diatom-specific growth limitation and changes in silicification (Si μm^{-2}), has largely eluded the field due to methodological constraints. Thus, whether sacrificing silicification to maintain division rate is a common adaptive strategy that influences population growth and succession within diverse natural diatom assemblages remains to be directly evaluated.

If the sequence of physiological responses to Si stress observed in culture is widely applicable to natural assemblages it would point to an r-selected mechanism whereby diatoms delay silicon growth limitation to maximize ultimate population size for a given pulse of $Si(OH)_4$. It would also suggest a shifting ecological role for diatoms based on the

degree of silicon stress. When the severity of silicon stress is sufficient to decrease diatom division rates, interspecific differences in silicon kinetics would influence both diatom-species (Paasche, 1973b; Tilman, 1977; Kilham and Tilman, 1979) and phytoplankton succession (Egge and Aksnes, 1992); these changes affect higher order consumers (Finney *et al.*, 2002), and the cycling of carbon (Tréguer *et al.*, 2017). Mild silicon stress, that stunts silica production rates and decreases silicification but does not alter division rate, would exert little bottom-up pressure on phytoplankton community structure. However, it could indirectly affect top-down pressure on the community because more lightly silicified cells are more susceptible to predation by a variety of zooplankton groups (Assmy *et al.*, 2013; Liu *et al.*, 2016; Zhang *et al.*, 2017) and changes in predation rate could affect the fate of diatom biomass and community structure. Additionally, mild silicon stress could have biogeochemical implications as decreased silicification reduces cell density, such cells would be more likely to remineralize and dissolve at shallow depths compared to heavily silicified individuals (Passow *et al.*, 2011).

Here, we use a recently developed method to directly quantify taxon-specific silicon stress in a coastal upwelling system. We examine the extent to which cells alter silicification and division rate with the increase of silicon stress that follows an initial nutrient injection. The results reveal high interspecific variation in the susceptibility of taxa to silicon stress but a shared physiological response to intensifying silicon stress.

Results

Environmental setting

Samples for incubation experiments were collected during the IrnBru (MV1405) cruise aboard the *R/V Melville* in July 2014. Water was collected during two transects off the California coast; each generally followed plumes of upwelled water that extended perpendicularly away from the coast (Fig. 1a) with the exceptions of station 2 in the northern transect and the transition to more oligotrophic water in station 5–7 along the southern transect. The recently upwelled water nearshore was cold with a high concentration of macronutrients, while the offshore water was warmer with lower nutrient concentrations. A more thorough description of the environmental conditions can be found in McNair *et al.* (2018). $[Si(OH)_4]$ concentration was highly correlated with $[NO_3^-]$ ($R = 0.84$, $p < 0.001$) and $[PO_4^{3-}]$ ($R = 0.96$, $p < 0.001$) with all three nutrients decreasing in concentration away from shore (McNair *et al.*, 2018). Along the northern transect $[Si(OH)_4]$ ranged from 21.2 μM near shore to 2.0 μM offshore; along the southern transect $[Si(OH)_4]$ ranged from 15.4 μM to 2.3 μM near shore to offshore, respectively (Fig. 1b).

Community-level changes in silica production

The degree of silicon stress was characterized by comparing the rate of silica production (V) in a +Si treatment, where sufficient $Si(OH)_4$ was added to saturate silica production rates (V_{+Si}), to the rate of silica production under ambient nutrient condition (V_{amb}), which was not amended with $Si(OH)_4$. The influence of community composition and environmental conditions on V_{amb} can be found in McNair *et al.* (2018). The ratio V_{+Si}/V_{amb} quantifies the degree to which silica production was limited by $[Si(OH)_4]$ under ambient conditions; larger

V_{+Si}/V_{amb} indicates more severe silicon stress and V_{+Si}/V_{amb} close to one indicates that the rate of silica production was insensitive to the additional $Si(OH)_4$ and thus was near maximum under ambient [$Si(OH)_4$].

Despite the large range of [$Si(OH)_4$] across both transects the bulk measurement of diatom community silica production from ^{32}Si measurements, showed the stress (V_{+Si}/V_{amb}) of the total diatom community was relatively constant among stations (Fig. 1b). The correlation between [$Si(OH)_4$] and V_{+Si}/V_{amb} in the northern transect was low and not significant ($R = -0.46$, $p = 0.36$). The correlation along the southern transect was positive and significant ($R = 0.83$, $p = 0.05$). On average, in the northern transect, community silica production rates increased by 43 ± 20% (S.E.) with the addition of 19 μM $Si(OH)_4$ (Fig. 1b). Along the southern transect, community silica production rates were similar, on average, in both treatments and only increased by 10 ± 15% (S.E.) with added $Si(OH)_4$.

Taxon-specific measures of silicon stress (measured with PDMPO and microscopy) were combined and averaged for each station then compared to the bulk-measurement (^{32}Si) of total community silicon stress (Fig. 1b). The averages were weighted by a taxon's contribution to silica production. Limited time and resources precludes making single-cell measurements for all taxa within a community as such, taxa were targeted for microscopy based on their likely contribution to silica production (i.e. abundant and/or large). Although only a fraction of the community was included in the weighted averages, the reconstructed estimates of community-level silicon stress at each station generally agreed with the direct total community measurements made with ^{32}Si (Fig. 1b). For the taxon-weighted community measurements, the addition of $Si(OH)_4$ increased community silica production by 27 ± 250% across stations on the northern transect and 45 ± 224% on the southern transect (Fig. 1b). The taxon-specific average silica production rates were not correlated with [$Si(OH)_4$] (northern transect, $R = -0.42$, $p = 0.41$, southern transect, $R = -0.17$, $p = 0.75$).

Taxon-specific changes in silica production, silicification, new frustule surface area, and division rate

The changes in silica production rates of individual taxa showed a wide range of responses to the addition of $Si(OH)_4$ (Fig. 2) even though the community response was relatively constant (Fig. 1b, white dots). Taxon-specific data were pooled across transects because there was no significant difference in the slopes of the regressions for any taxon-specific rate parameter with [$Si(OH)_4$] between transects including the Si uptake ratio (V_{+Si}/V_{amb}, $F = 0.12$, $p = 0.73$), change in silicification (Z_{+Si}/Z_{amb}, $F = 0.01$, $p = 0.90$), the surface area of new frustule created during the incubation (SA_{new+Si} /$SA_{new-amb}$, $F = 1.01$, $p = 0.31$), or division rate (μ_{+Si}/μ_{amb}, $F = 1.16$, $p = 0.29$). Within a station, taxa exhibited values of V_{+Si}/V_{amb} from ~1 to ~3 (Fig. 2a). The variability of V_{+Si}/V_{amb} among taxa generally increased as [$Si(OH)_4$] decreased.

Taxon-specific V_{+Si}/V_{amb} varied among stations as well (Sup. Table 1). Some taxa, such as *Skeletonema* sp. and *Chaetoceros spp.* <20 μm appeared Si-replete across the gradient in [$Si(OH)_4$], with V_{+Si}/V_{amb} generally close to one (Fig. 2a, Sup. Table 1). Silica production rates for other taxa, such as the centrics (*Thalassiosira*-like cells) and *Chaetoceros spp.* >20

μm were more silicon stressed, showing a nearly 3-fold silica production increase in response to added $Si(OH)_4$ (Fig. 2a). The relative interspecific sensitivity to silicon stress was examined by evaluating the fraction of stations where each species exhibited significant Si stress. The number of instances where a specific taxon's V_{+Si}/V_{amb} was greater than 1.3 (i.e. one plus the average standard error of V_{+Si}/V_{amb}, which was 30%) was divided by the number of stations for which we had data for that taxon, to quantify the fraction of stations where limitation was observed for each taxon (Fig. 3). By this metric silica production by *Fragilariopsis sp., Skeletonema sp.*, and *Chaetoceros spp.* <20 μm was least often silicon stressed, while *Proboscia alata, Chaetoceros spp.* >20 μm and *F. pseudonana* was most often silicon stressed. The remaining taxon spanned a continuum.

The amount of silica that a cell produces over a given time is the mathematical product of the surface area of the new frustule created (SA_{new}, μm^2) and the silicification (Z, Si μm^{-2}) of the new frustule. On average SA_{new+Si} was 8% more than $SA_{new-amb}$ but was variable within a taxon at a given station with no trend in magnitude or variance with $[Si(OH)_4]$ (Fig. 2b). Z increased within the +Si treatment by an average of 36% across taxa and stations (Fig. 2c). Similar to V_{+Si}/V_{amb}, the variability in Z_{+Si}/Z_{amb} generally increased among taxa with decreasing $[Si(OH)_4]$. The ~2-fold average increase in Z_{+Si}/Z_{amb} with declining $[Si(OH)_4]$ was less than observed for V_{+Si}/V_{amb} as expected (see explanation below), except for the high value for centric diatoms at ~10 μM $Si(OH)_4$ (Fig. 2c).

Generally, division rate was altered little with additional $Si(OH)_4$. However, *P. alata* and *Chaetoceros spp.* >20 μm, which were the taxa most frequently silicon stressed (Fig. 3) showed a 0.5 to 2-fold increase in growth rate with added Si when ambient $Si(OH)_4$ was <10 μM (Fig. 2d). Division rate was estimated by the PDMPO-labelling patterns of partially, half, and fully labeled cells as in McNair *et al.* (2018). Division rate generally ranged from one to three divisions per day across taxa (McNair *et al.*, 2018).

The relationship between silica production, silicification, surface area and division rate

The coordination of physiological responses (i.e. silicification (Z), new surface area produced (SA_{new}), growth rate (μ)) as a function of silicon stress were examined among all taxa (Fig. 4). As described in the methods, all regressions were forced through the coordinate (1, 1). The regressions for both Z and SA_{new} with the silicon stress index (V_{+Si}/V_{amb}) were significant, while that between μ and V_{+Si}/V_{amb} was not:

$$\text{Silicification: } Z_{+Si}/Z_{amb} = 0.58 \pm 0.06 \times \left(V_{+Si}/V_{amb}\right) + 0.42 \; (p < 0.001)$$

$$\text{New surface area: } SA_{new+Si}/SA_{new-amb} = 0.29 \pm 0.04 \times \left(V_{+Si}/V_{amb}\right) + 0.71 \; (p < 0.001)$$

$$\text{Growth: } \mu_{+Si}/\mu_{amb} = 0.08 \pm 0.05 \times \left(V_{+Si}/V_{amb}\right) + 0.92 \; (p = 0.12)$$

Mathematically changes in silicification and the surface area of new frustule created contribute equally to the rate of silica production, such that the degree of silicon stress can theoretically be related to changes in Z and SA_{new} by:

$$V_{+Si}/V_{amb} = \left(SA_{new+Si}/SA_{new\text{-}amb}\right) \times \left(Z_{+Si}/Z_{amb}\right) \quad (1)$$

This equation holds for the regression lines in Figure 4 such that the product of Z_{+Si}/Z_{amb} and $SA_{new+Si}/SA_{new\text{-}amb}$ well predicts the measured V_{+Si}/V_{amb} (slope = 1.001, $R^2 = 0.93$). The slope of the relationship between silicification and the silicon stress index was nearly twice that for the new surface area, indicating that the dominant response across taxa to increasing silicon stress was a reduction in cell silicification.

Silicon stress effects on contribution of taxa to community silica production and abundance

To better understand the role of $[Si(OH)_4]$ in regulating community silica production and community composition, the fractional contribution of each taxon to total silica production and to total cell abundance was compared in the ambient and +Si treatments (Fig. 5). Across taxa the slope of the reduced major axis regression between a taxon's contribution to silica production (Fig. 5a) in the ambient and +Si treatment was close to unity, 0.97 ± 0.10 (95% C.I.) ($R^2 = 0.91$) despite individual taxa exhibiting a two- to three-fold shift in silica production rate between treatments. This signifies that a taxon's contribution to community silica production was essentially unaltered, even though total community silica production rates generally increased with the addition of $Si(OH)_4$. Similarly, the fractional abundance of taxa at the end of the incubation, which was calculated using division rate and initial cell abundance (McNair *et al.*, 2018), was not significantly different between the ambient and +Si treatment (Fig. 5b). The slope of the reduced major axis regression for the abundance measures was 1.01 ± 0.08 (S.E.) ($R^2 = 0.96$).

Discussion

Prolonged rapid growth in dynamic ocean regions make diatoms one of the most productive primary producers globally. Our field data show for the first time that the decrease in silicification in lieu of decreased growth rate first inferred in laboratory experiments 45 years ago, is a coping mechanism employed by multiple taxa within natural diatom communities. Both the data presented here and those from culture studies (Guillard *et al.*, 1973; Paasche, 1975) find that diatoms first respond to reductions in silicon availability by thinning their frustules, which minimizes the impact of diminished Si uptake rates on division rates (Fig. 4). The more lightly silicified cells observed in the ambient treatment indicate that, as silica production rates became limited *in situ* by $[Si(OH)_4]$, cells decreased their silicon quota such that the experimental addition of $Si(OH)_4$, i.e. release from silicon stress, restored maximum silica production rates and maximum silicification during the 24 h incubation. This is direct and quantitative field evidence that diatoms maximize growth rate at the expense of other aspects of cell physiology, specifically their frustule properties. Such a response is consistent with the r-strategy of diatom adaptation whereby they are able to

respond quickly to inputs of nutrients (Sommer, 1983) and maintain high growth rates as nutrients decrease (this study), and thus thrive in turbulent environments (Margalef, 1978). Along with their intrinsic high division rates, the prioritization of cell division rate produces the maximum number of individuals for a given pulse of $Si(OH)_4$ favoring persistence in environments with episodic nutrient input.

Diatom division rates across the transects significantly correlated with macronutrient concentrations (McNair *et al.*, 2018). However, the results presented here imply that decreasing silicic acid, and thus increasing silicon stress, was not the cause of observed decreases in division rates (Fig. 4). Growth limitation by factors besides silicon (light, iron, nitrate, etc.) often inversely correlate with silicification because decreased growth rate gives a cell more time to acquire silicon, which could result in a fully silicified cell even when $[Si(OH)_4]$ is low (Claquin *et al.*, 2002). All other things being equal, decreasing growth rate would decrease silicon stress (V_{+Si}/V_{amb}). Within the dataset, silicon stress generally increased and silicification decreased with decreasing $Si(OH)_4$ (Fig. 2). This suggests that any decreases in growth did not slow the cell cycle sufficiently to allow cells with less than maximum Si uptake rates to acquire enough silicon to produce fully silicified frustules in ambient $[Si(OH)_4]$. This ability to produce less silicified frustules in favor of progressing through the cell cycle enabled most taxa in this study to avoid silicon growth limitation for $[Si(OH)_4]$ down to 2 μM.

The lack of decrease in growth rate with increasing silicon stress is likely reflective of the ambient $[Si(OH)_4]$ not being sufficiently low to induce the severe silicon stress that would overcome the compensatory mechanism of frustule thinning and lower division rates. In culture, diatoms are capable of thinning their frustules by a factor of 3–4 in response to low $[Si(OH)_4]$ (Guillard *et al.*, 1973; Paasche, 1975; Brzezinski *et al.*, 1990) suggesting that V_{+Si}/V_{amb} would have to exceed a value of 3–4 before reductions in division rate would be expected. In our dataset V_{+Si}/V_{amb} was < 3 (Fig. 4) and direct quantifications of cell thinning were generally less than a factor of two (Fig. 4). By both criteria, the observed minimal impact to division rates was expected.

Quantitative data showing the lower sensitivity of growth rate than silica production rate to changes in $Si(OH)_4$ availability (Fig. 2) provides the opportunity to quantitatively evaluate another aspect of diatom silicon physiology using the response of multiple co-occurring species in nature. An explicit outcome of the thinning of frustules in response to diminishing $[Si(OH)_4]$ is that the half-saturation for growth (K_μ) is less than that for silica production (K_s) (Martin-Jézéquel *et al.*, 2000). Using the kinetic equations for growth (Monod (Monod, 1942)) and silica production (Michaelis-Menten (Michaelis and Menten, 1913)) we can estimate the relative magnitude of the average K_s and average K_μ for taxa in our dataset. By solving both equations for $[Si(OH)_4]$, the setting them equal to each other, and solving for μ_m/μ (Sup. Info.) we form a relationship with K_μ/K_s:

$$\frac{\mu_m}{\mu} = \frac{K_\mu}{K_s}\left(\frac{V_m}{V}\right) - \left(\frac{K_\mu}{K_s} - 1\right) \quad (2)$$

where μ_m and μ are approximated by the measured μ_{+Si} and μ_{amb}, respectively and V_m and V are approximated by V_{+Si} and V_{amb}, respectively. This equation is in the same form as the regressions from Figure 4 ($\mu_{+Si}/\mu_{amb} = 0.08 \pm 0.05 \times (V_{+Si}/V_{amb}) + 0.92$; $p = 0.12$) such that the slope of V_{+Si}/V_{amb} versus μ_{+Si}/μ_{amb} is the ratio of K_μ to K_s. The slope of this relationship (0.08) was significantly less than one (t-test, t ratio 15.36, $p < 0.001$). Assuming the Monod and Michaelis-Menten models are accurate for field diatoms, this directly confirms that K_μ is considerably less than K_s and is the underlying reason for the quantitatively measured decoupling of silica production and division rates.

Ecological and biogeochemical implications of silicon stress

Shifting silicon availability was not a dominant force in shaping diatom community composition. Increased availability of $Si(OH)_4$ minimally affected division rates such that at the end of the 24-hr incubation the fractional distribution of taxa was not different in the ambient and +Si samples (Fig. 5). However, small changes in growth compound over time so any difference in growth rate between the ambient and +Si treatments may be more pronounced on longer timescales. In environments where the ambient $[Si(OH)_4]$ is very low, e.g. <0.5 μM observations in the California Current (Krause *et al.*, 2015) or Mississippi River Plume (Nelson and Dortch, 1996), our results predict that $[Si(OH)_4]$ could severely limit diatom growth and affect community structure on shorter time scales.

Given that silicon stress did not affect division rate, the absence of changes to community composition over our one-day incubations was expected (Fig. 5b). However, community and taxon-specific silica production rates were consistently higher in the +Si treatment (Fig. 1b). This combined with the variability of silicon stress among taxa at a station suggested that the distribution of silica production among diatom taxa would be altered with decreasing $[Si(OH)_4]$. Yet, there was not a significant difference between treatments in the fractional amount of silica produced by taxa (Fig 5a). The changes in silica production rate that occurred with increased $Si(OH)_4$ were too small to overcome the large initial differences in fractional contributions to silica production.

While community dynamics were not altered with silicon stress, the coordinated decrease in silicification likely affects regional nutrients cycles and food-web dynamics. More lightly silicified frustules result in decreased cell density which decreases sinking speed. The potential decrease in sinking speed can be calculated using the modified Stokes equations from Miklasz and Denny (2010) assuming decreased silicification was the only physiological change induced with silicon stress. Across the size range of cells in this study sinking speeds would decrease 15–35% for $Z_{+Si}/Z_{amb} = 1.5$ which would increase the likelihood for diatom-bound nutrients being retained in the surface ocean (Tréguer *et al.*, 2017). Changes in silicification could additionally affect flows of energy through the food-web. Studies that measured changes in grazing pressure with changes in silicification found that decreasing silicification led to increased predation from microzooplankton (Zhang *et al.*, 2017) and copepods (Liu *et al.*, 2016). The ratios of silicification from those studies (Z_{+Si}/Z_{amb}~1.4 and ~2, respectively) falls within the range observed here, suggesting that top-down forces may become an increasingly important loss for diatoms that are silicon stressed.

The consistent decrease in silicification (Si μm^{-2}) in response to silicon stress with the maintenance of division rate confirms the prevalence of an adaptive strategy in nature that facilitates the formation of large diatom blooms in episodically nutrient-rich habitats. Because division rates were generally unaltered by [$Si(OH)_4$] across taxa, silicon stress had little influence on community composition. The impact on taxon-specific contribution to community silica production was also small in our incubations, despite interspecific differences in the degree of silicon stress among co-occurring diatoms. In these environments with intermittent nutrient infusions diatom community composition is more likely a reflection of interspecific differences in maximum, unrestricted division rates as well as differential grazing pressure rather than a reflection of cells best adapted to low nutrient conditions. Any effects of resource limitation on community succession is likely consequence of taxonomic-specific responses to resources other than dissolved silicon. The decrease of frustule strength caused by decreased silicification could make cells more susceptible to predation and more likely to fuel regenerative production, which together alter food web dynamics and regional nutrient cycles. Yet, the increased risk of predation is opposed by the r-selected strategy of maximizing population size for a given pulse of silicon; thereby favoring diatom persistence in pulsed resource environments such as coastal upwelling systems.

Experimental Procedures

Sample collection

Data for this study was collected during the IrnBru (MV1405) cruise aboard the *R/V Melville* in July 2014 along two transects off the California coast. The northern transect extended ~100 km southwest from Cape Blanco, Oregon (USA) and the southern transect extended ~200 km west from Point Arena, California (USA) (Fig. 1a). Macronutrient and biogenic silica ($bSiO_2$) samples were collected along both transects as described in (McNair *et al.*, 2018).

At each station, silica production rates, growth rates, and silicification were measured in incubations of paired ‘ambient’ and ‘+Si’ treatments to characterize the degree of silicon stress. Water for the incubations was collected at roughly two-hour intervals while the ship was underway (Fig. 1a) using a surface-towed, trace metal clean, water pump, (i.e. the Geo Fish, (Bruland *et al.*, 2005)). The fluorescent tracer, PDMPO [2-(4-pyridyl)-5-((4-(2-dimethylaminoethylamino-carbamoyl)methoxy)phenyl)oxazole] was added to each pair of bottles to a final concentration of 0.158 μM. The ambient treatment was not altered further. The +Si treatment was spiked with a Chelex-cleaned sodium metasilicate stock solution such that the final concentration was 19 μM greater than the ambient of [$Si(OH)_4$]. To measure the silica production rates of the total diatom community at each station, an additional pair of ambient and +Si bottles were spiked with the radioisotope ^{32}Si (15,567 Bq μg^{-1}). 261 Bq of ^{32}Si was added to samples from the northern transect and 293 Bq of ^{32}Si was added to samples from the southern transect.

All the bottles were incubated for 24 h in deck-board, flow-through incubators with circulation surface seawater to maintain temperature and processed as in McNair *et al.*, (2018). PDMPO fluorescence was used to estimate cell-specific silica production rates,

growth rates and silicification as described in McNair *et al.*, (2018). Samples for ^{32}Si production rate measurements were filtered through 25 mm diameter, 1.2 μm pore size, filters, air dried and mounted on planchettes (Krause *et al.*, 2011). ^{32}Si activity was measured using low-level beta detection after aging samples into secular equilibrium between the ^{32}Si and its short-lived daughter isotope, ^{32}P, and production rates calculated as in (Krause *et al.*, 2011).

Metrics of Si stress

A normalization procedure was used to compare the responses to silicon stress among taxa as prior results indicated silica production rates spanned three orders of magnitude (McNair *et al.*, 2018). The relative degree of silicon stress for each taxon was quantified by comparing the rate of silica production in the +Si treatment to the rate of silica production in the ambient treatment (ρ_{+Si}/ρ_{amb}) where both measures are in units of mol Si cell^{-1} h^{-1}. Assuming the silica content for all cells of a given taxa was the same at the start of the incubation in both the ambient and +Si treatments, the ratio of ρ_{+Si}/ρ_{amb} = (V+Si$\cdots$bSiO$_2$) ÷ (Vamb bSiO$_2$) is equivalent to V_{+Si}/V_{amb}

The experimental addition of $Si(OH)_4$ in the +Si treatment is assumed to relieve cells from any silicon stress that may be occurring in the ambient conditions and thus V_{+Si}/V_{amb} approximates V_m/V (eq. 1). The normalization places the response of all taxa on the same relative scale that can be directly related to changes in silicon production kinetics (eq. 1). V_{+Si}/V_{amb} scales linearly with the degree of Si stress, with larger values indicating greater stress. Similarly, changes in measures of silicification (Z), new frustule SA production rate (SA_{new}), and growth rate (μ) were normalized by dividing the value of each parameter in the +Si treatment by the paired measurement in the ambient treatment.

Data quality control

The taxon-specific data for silica production rate, growth rate, and silicification are inherently variable. Time and resources limit the number of cells that can be imaged on the confocal microscope for each sample. This constrains the number of cells included in the averages for each taxon and results in a large standard error (S.E.) for the mean response of a taxon when only a few individuals are imaged. Silica production rates can vary widely within a genus or taxonomic group adding to the variance of averages for taxonomic groups that are resolved only to the genus level. Variation also arises from intraspecific variability among cells of the same species. For instance, *Fragilariopsis pseudonana* had silica production rates that spanned an order of magnitude within a station. This variation is consistent with the findings of Durkin et al. (2012), who reported an order of magnitude range in PDMPO fluorescence in *Fragilariopsis sp.* (5 μm) from the subarctic Pacific when quantifying fluorescence with a flow cytometer, which analyzes significantly more individuals. The necessary grouping of multiple species into the taxonomic groups reported here such as “centrics” and “*Pseudo-nitzschia spp.*” compounds apparent intraspecific differences. On average, the S.E. across measurements for different taxon and taxonomic groups was 36% of the mean for V_{+Si}/V_{amb}, 19% for Z_{+Si}/Z_{amb}, 26% $SA_{new+Si}/SA_{new-amb}$ and 12% for μ_{+Si}/μ_{amb}.

To reduce the influence of highly variable data points in our analyses, the data were filtered using two objective criteria: the number of cells included in the average needed to be greater than four in both treatments and the magnitude of the S.E. of V_{+Si}/V_{amb} had to be less than 70% of the average. This removed 23 out of 61 data points across the thirteen stations. After applying these criteria, the average S.E. relative to the mean decreased to 30% for V_{+Si}/V_{amb}, 16% of for Z_{+Si}/Z_{amb}, 23% for $SA_{new+Si}/SA_{new-amb}$, and increased to 13% for μ_{+Si}/μ_{amb}.

Statistics

Simple linear regressions using JMP12 were used to relate relative changes in growth rate, silicification, and the rate of new frustule surface area production to changes in relative silica production rate. Reduced major axis regressions were not used in this instance because of the asymmetric relationship between variables (Smith, 2009), i.e. X and Y variables were not interchangeable because the intent was to investigate physiological response (Z_{+Si}/Z_{amb}, $SA_{new+Si}/SA_{new-amb}$, μ_{+Si}/μ_{amb}) as a function of Si stress (V_{+Si}/V_{amb}). An analysis of covariance (ANCOVA) was used to test for differences in the regressions between transects (run in JMP 12). A reduced major axis regression was used to compare the relative contribution of taxa to community silica production and fractional abundance in the ambient versus the +Si treatment. This analysis was preformed using the R package lmodel2.

Under the assumption that the Si addition in the +Si treatment raised each metric to their physiological maximum, the relationship between the silicon stress metric (V_{+Si}/V_{amb}) and silicification (Z_{+Si}/Z_{amb}), new frustule SA ($SA_{new+Si}/SA_{new-amb}$), and growth rate (μ_{+Si}/μ_{amb}) should all mathematically converge at x, y = 1, 1 at infinite [$Si(OH)_4$]. The linear regressions were forced through (1, 1) by subtracting each datum from a value of one, e.g. $1-Z_{+Si}/Z_{amb}$, which transposed the coordinate (1, 1) to (0, 0). Then least squares linear regression was applied to the relationship between the transformed physiological metric and the transformed silicon stress metric (V_{+Si}/V_{amb}) while forcing the intercept of the regression through zero. The resulting equation was translated back to the original parameter space giving a final equation for the line in the form:

$$V_{+Si}/V_{ambi} = m^* A_{+Si}/A_{amb} + (1 - m) \quad (3)$$

Where A is either Z, SA_{new} or μ and m is the slope of the line from the linear regression that was forced through zero.

Supplementary Material

Refer to Web version on PubMed Central for supplementary material.

Acknowledgements

We thank Ken Bruland for extending the opportunity to participate in this cruise as well as the crew of the *R/V Melville* for their dedication and assistance and the science party, especially J. Jones, for making the cruise successful. H. Moeller, C. Carlson, M. Maniscalco, I. Closset, and N. Huynh provided helpful feedback and suggestions that shaped this manuscript. This research was funded by the National Science Foundation grant

OCE-1155663 (awarded to JWK and MAB), microscopy instrumentation was supported by the National Institute of Health grant 1 S10 OD010610–01A1 (awarded to the NRI-MCDB Microscope Facility).

References

Assmy P, Smetacek V, Montresor M, Klaas C, Henjes J, Strass VH, et al. (2013) Thick-shelled, grazer-protected diatoms decouple ocean carbon and silicon cycles in the iron-limited Antarctic Circumpolar Current. Proc. Natl. Acad. Sci 110: 20633–20638. [PubMed: 24248337]

Bruland KW, Rue EL, Smith GJ, and DiTullio GR (2005) Iron, macronutrients and diatom blooms in the Peru upwelling regime: brown and blue waters of Peru. Mar. Chem 93: 81–103.

Brzezinski MA, Olson RJ, and Chisholm SW (1990) Silicon availability and cell-cycle progression in marine diatoms. Mar. Ecol. Prog. Ser 67: 83–96.

Claquin P, Martin-Jézéquel V, Kromkamp JC, Veldhuis MJW, and Kraay GW (2002) Uncoupling of silicon compared with carbon and nitrogen metabolisms and the role of the cell cycle in continuous cultures of Thalassiosira pseudonana (Bacillariophyceae) under light, nitrogen, and phosphorus control. J. Phycol 38: 922–930.

Durkin C. a., Marchetti A, Bender SJ, Truong T, Morales R, Mock T, and Virginia Armbrust E (2012) Frustule-related gene transcription and the influence of diatom community composition on silica precipitation in an iron-limited environment. Limnol. Oceanogr 57: 1619–1633.

Egge JK and Aksnes DL (1992) Silicate as regulating nutrient in phytoplankton competition. Mar. Ecol. Prog. Ser 83: 281–289.

Finney BP, Gregory-Eaves I, Douglas MSV, and Smol JP (2002) Fisheries productivity in the northeastern Pacific Ocean over the past 2,200 years. Nature 416: 729–733. [PubMed: 11961553]

Guillard RRL, Kilham P, Jackson TA, and Jackson, G.R.R.L.K.P. and T.A. (1973) Kinetics of silicon-limited growth in the marine diatom Thalassiosira pseudonana Hasle and Heimdal (= Cyclotella nana Hustedt). J. Phycol 9: 233–237.

Kilham P and Tilman D (1979) The importance of resource competition and nutrient gradients for phytoplankton ecology. Arch. Hydrobiol. (Beih): Ergebn. Limnol 13: 110–119.

Kooistra WHCF, Gersonde R, Medlin LK, and Mann DG (2007) The Origin and Evolution of the Diatoms: Their Adaptation to a Planktonic Existence In, Evolution of Primary Producers in the Sea. Elsevier, pp. 207–249.

Krause JW, Brzeinski MA, and Jones JL (2011) Application of low-level beta counting of ^{32}Si for the measurement of silica production rates in aquatic environments. Mar. Chem 127: 40–47.

Krause JW, Brzezinski MA, Goericke R, Landry MR, Ohman MD, Stukel MR, and Taylor AG (2015) Variability in diatom contributions to biomass, organic matter, production and export across a frontal gradient in the California Current Ecosystem. Jounral Geophys. Res. Ocean 120: 1–16.

Liu H, Chen M, Zhu F, and Harrison PJ (2016) Effect of Diatom Silica Content on Copepod Grazing, Growth and Reproduction. Front. Mar. Sci 3: 89.

Lochte K, Ducklow HW, Fasham MJR, and Stienen C (1993) Plankton succession and carbon cycling at 47N and 20W during the JGOFS North Atlantic Bloom Experiment. Deep. Res. II 40: 91–114.

Malviya S, Scalco E, Audic S, Vincent F, Veluchamy A, Bittner L, et al. (2016) Insights into global diatom distribution and diversity in the world's ocean. Proc. Natl. Acad. Sci 113: E1516–E1525. [PubMed: 26929361]

Margalef R (1978) Life-forms of phytoplankton as survival alternatives in an unstable environment. Ocean. Acta 1: 493–509.

Martin-Jézéquel V, Hildebrand M, Brzezinski MA, Martin-Jezequel V, Hildebrand M, Brzezinski MA, and Martin-Jézéquel V (2000) Silicon metabolism in diatoms: implications for growth. J. Phycol 36: 821–840.

McNair HM, Brzezinski MA, Till CP, and Krause JW (2018) Taxon-specific contributions to silica production in natural diatom assemblages. Limnol. Oceanogr 63: 1056–1075. [PubMed: 29937577]

Merico A, Tyrrell T, Lessard EJ, Oguz T, Stabeno PJ, Zeeman SI, and Whitledge TE (2004) Modelling phytoplankton succession on the Bering Sea shelf: Role of climate influences and trophic

interactions in generating Emiliania huxleyi blooms 1997–2000. Deep. Res. Part I Oceanogr. Res. Pap 51: 1803–1826.

Michaelis L and Menten MML (1913) Die kinetik der Inverinwirkung. Biochem. Z 49: 333–369.

Miklasz KA and Denny MW (2010) Diatom sinking speeds: Improved predictions and insight from a modified Stoke's law. Limnol. Oceanogr 55: 2513–2525.

Monod J (1942) Recherches sur la croissance des cultures bacteriennes. 2nd ed Herman, Paris.

Nelson DM, Brzezinski MA, Sigmon DE, and Franck VM (2001) A seasonal progression of Si limitation in the Pacific sector of the Southern Ocean. Deep. Res. II 48: 3973–3995.

Nelson DM and Dortch Q (1996) Silicic acid depletion and silicon limitation in the plume of the Mississippi River: evidence from kinetic studies in spring and summer. Mar. Ecol. Prog. Ser 136: 163–178.

Nelson DM and Tréguer P (1992) Role of silicon as a limiting nutrient to Antarctic diatoms: evidence from kinetic studies in the Ross Sea ice-edge zone. Mar. Ecol. Prog. Ser 80: 255–264.

Nelson DM, Treguer P, Brzezinski MA, Leynaert A, and Queguiner B (1995) Production and dissolution of biogenic silica in the ocean : Revised global estimates, comparison with regional data and relationship to biogenic sedimentation. Global Biogeochem. Cycles 9: 359–372.

Paasche E (1975) Growth of the plankton diatom Thalassiosiranordenskioeldii Cleve at low silicate concentrations. J. Exp. Mar. Bio. Ecol 18: 173–183.

Paasche E (1973a) Silicon and the Ecology of Marine Plankton Diatoms . I . Thalassiosira pseudonana (Cyclotella nana) Grown in a Chemostat with Silicate as Limiting Nutrient. Mar. Biol 19: 117–126.

Paasche E (1973b) Silicon and the Ecology of Marine Plankton Diatoms . II . Silicate-Uptake Kinetics in Five Diatom Species. Mar. Biol 19: 262–269.

Passow U, French MA, and Robert M (2011) Biological controls on dissolution of diatom frustules during their descent to the deep ocean: Lessons learned from controlled laboratory experiments. Deep Sea Res. Part I Oceanogr. Res. Pap 58: 1147–1157.

Sieracki ME, Verity PG, Stoecker DK, and Seracki ME (1993) Plankton community response to sequential silicate and nitrate depletion during the 1989 North Altlantic spring bloom. Deep. Res. II 40: 213–225.

Smith RJ (2009) Use and misuse of the reduced major axis for line-fitting. Am. J. Phys. Anthropol 140: 476–486. [PubMed: 19425097]

Sommer U (1983) Nutrient competition between phytoplankton species in multispecies chemostat experiment. Arch. Hydrobiol 96: 399–416.

Tilman D (1977) Resource competition between planktonic algae: an experimental and theoretical approach. Ecology 58: 338–348.

Tréguer P, Bowler C, Moriceau B, Dutkiewicz S, Gehlen M, Aumont O, et al. (2017) Influence of diatom diversity on the ocean biological carbon pump. Nat. Geosci 11:.

Zhang S, Liu H, Ke Y, and Li B (2017) Effect of the Silica Content of Diatoms on Protozoan Grazing. Front. Mar. Sci 4:.

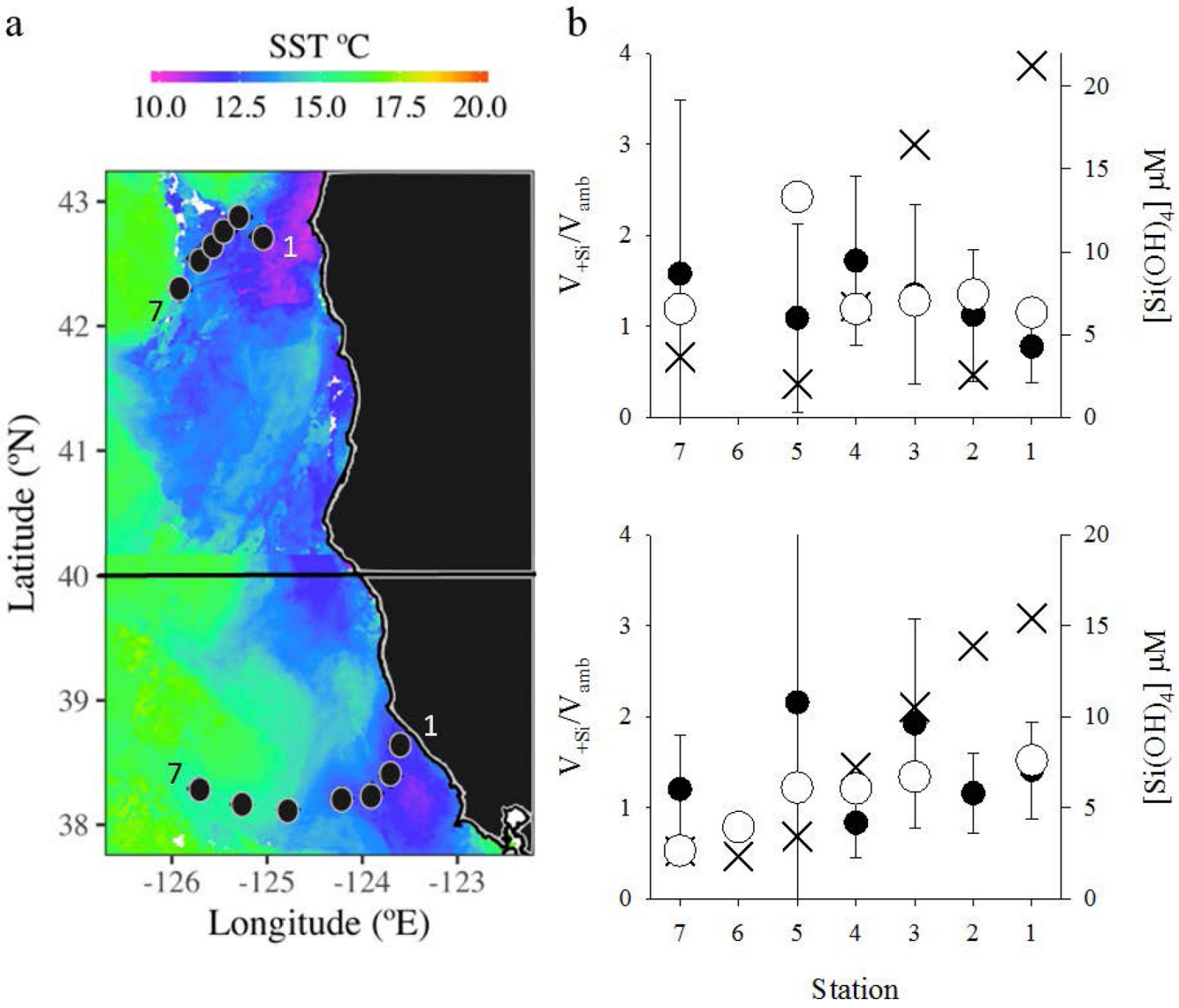

Figure 1:

(a) MODIS 8-day composite of sea surface temperature (SST) for the northern and southern transect with stations denoted as circles, station 1 was closest to shore and 7 was farthest offshore. The black line at 40° latitude breaks the 8-day composite centered on July 20, 2014 for the northern transect from the composite centered on July 7, 2014 for the southern transect. Map adapted from McNair *et al.*, (2018). (b) Relative degree of silicon stress (V_{+Si}/V_{amb}) along the northern transect (top panel) and along the southern transect (bottom panel). White circles denote total community production as measured with ^{32}Si tracer, black circles denote average, weighted, taxa-specific silica production from the fraction of the community measured with PDMPO. Error bars represent standard error. Silicic acid concentration (x's) in µM.

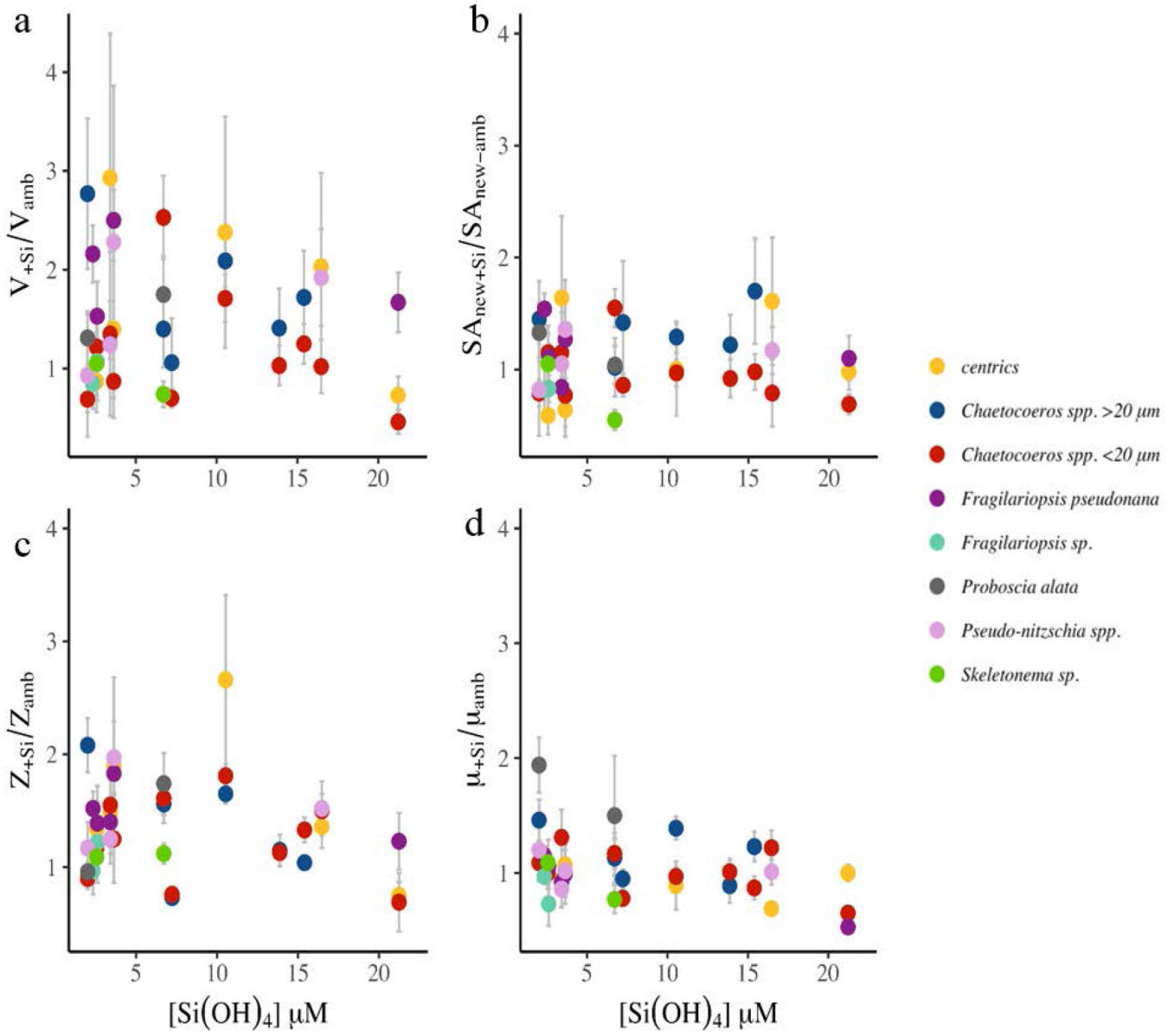

Figure 2:

Relative change in taxon-specific physiological parameters with silicic acid concentration. (a) The relative increase in silica production rate (b) the relative increase in new frustule SA, (c) the relative increase in silicification and (d) the relative change in growth rate. Colors correspond to taxa as shown in the key; *Thalassiosira*-like cells make up the centrics group. The ratio is between the ambient and enhanced treatments for taxa, the x-axis is the concentration of silicic acid in µM in the ambient condition.

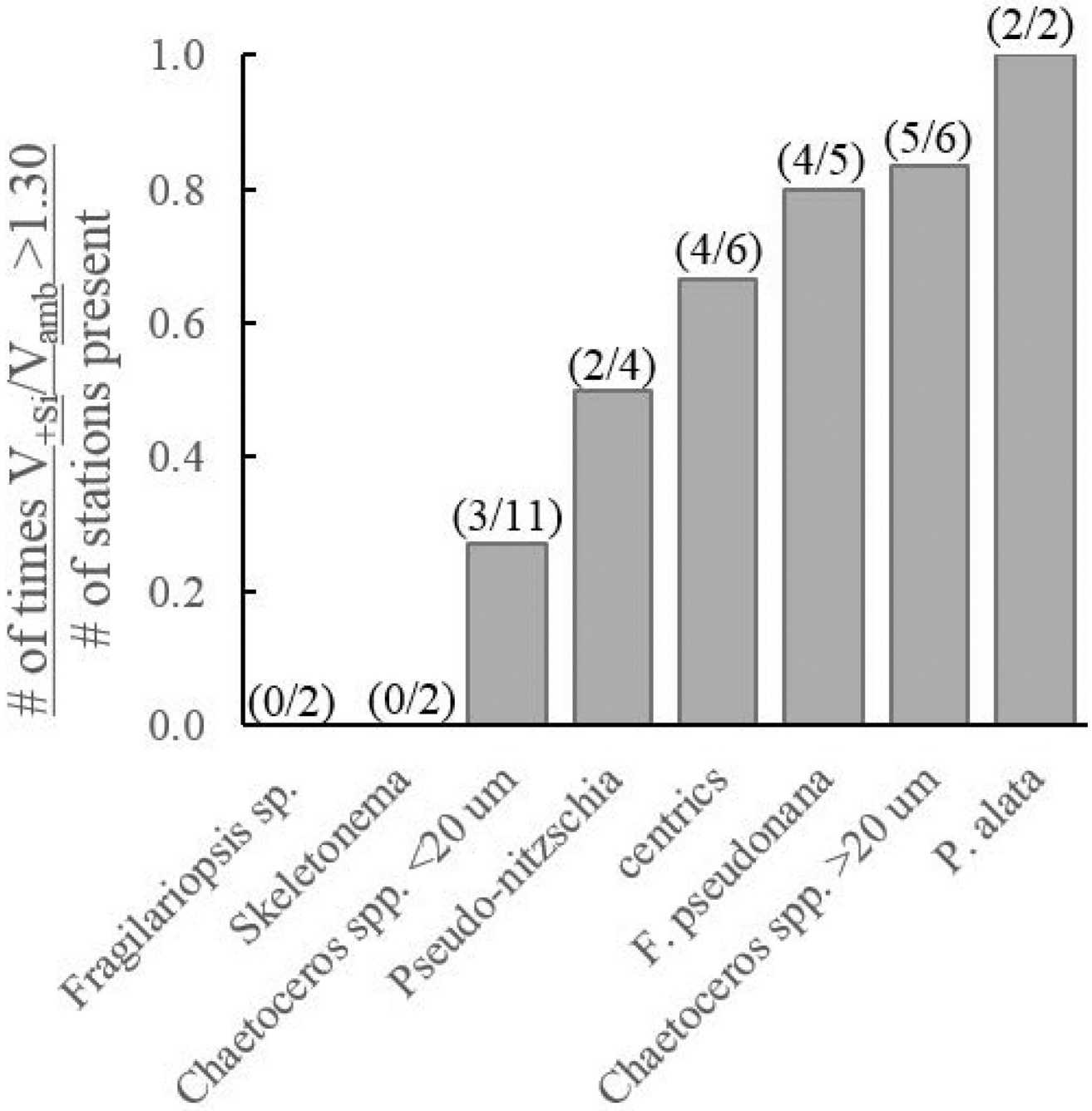

Figure 3:

Relative stress levels for taxa across all stations. The average standard error of V_{+Si}/V_{amb} among taxa was ~30% thus, a taxon was considered notably stressed when V_{+Si}/V_{amb} >1.3. The bars depict the quotient of the number of occurrences of V_{+Si}/V_{amb} greater than 1.3 divided by the number of stations in which that taxon was present, counts are given over each bar in parentheses.

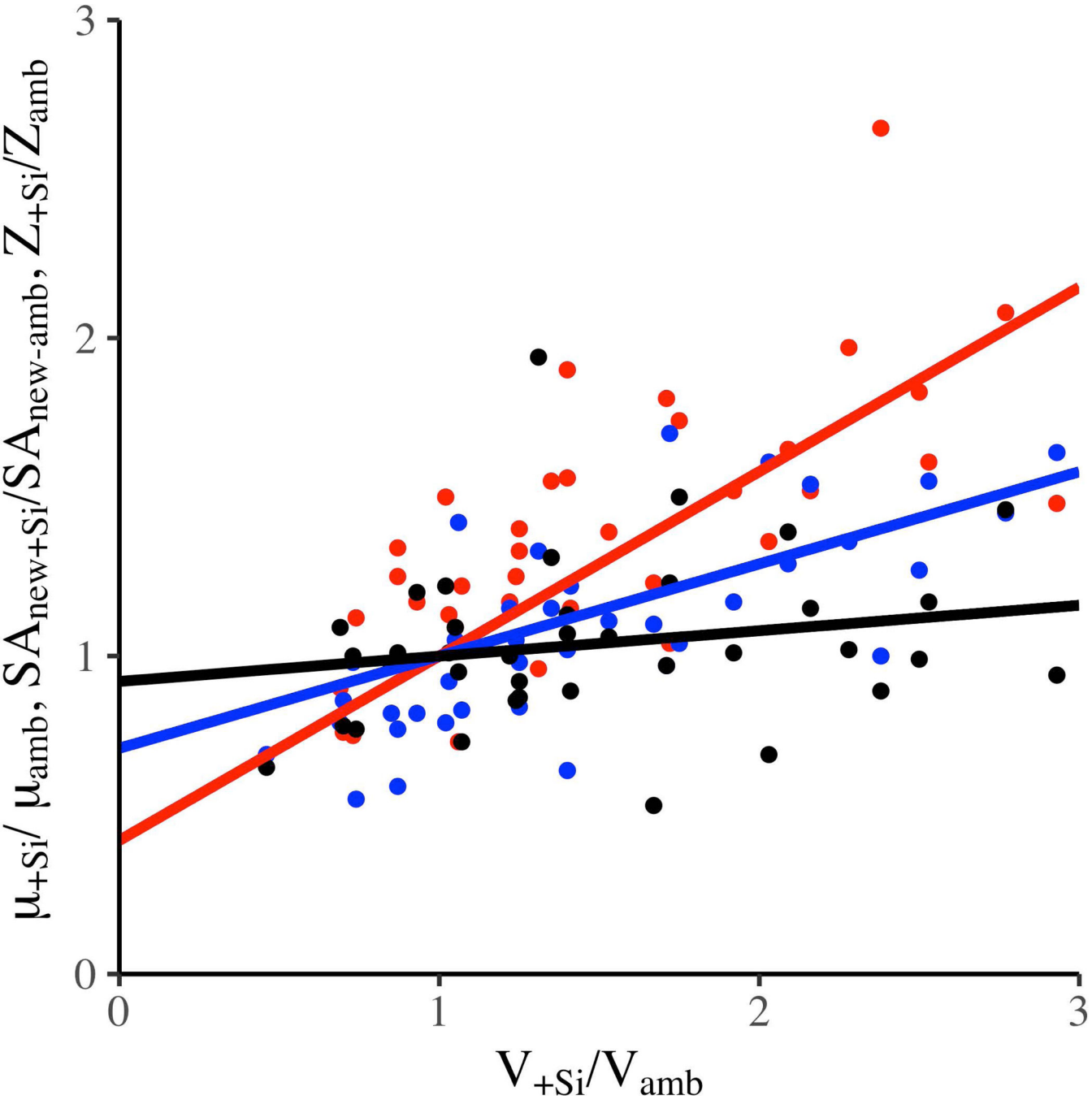

Figure 4:

Relationships between changes in silicification (Z, red), new frustule SA (SA_{new}, blue) and growth rate (μ, black) with increased silicon limitation (V_{+Si}/V_{amb}). All least squares linear regressions were forced through (x, y) = (1, 1).

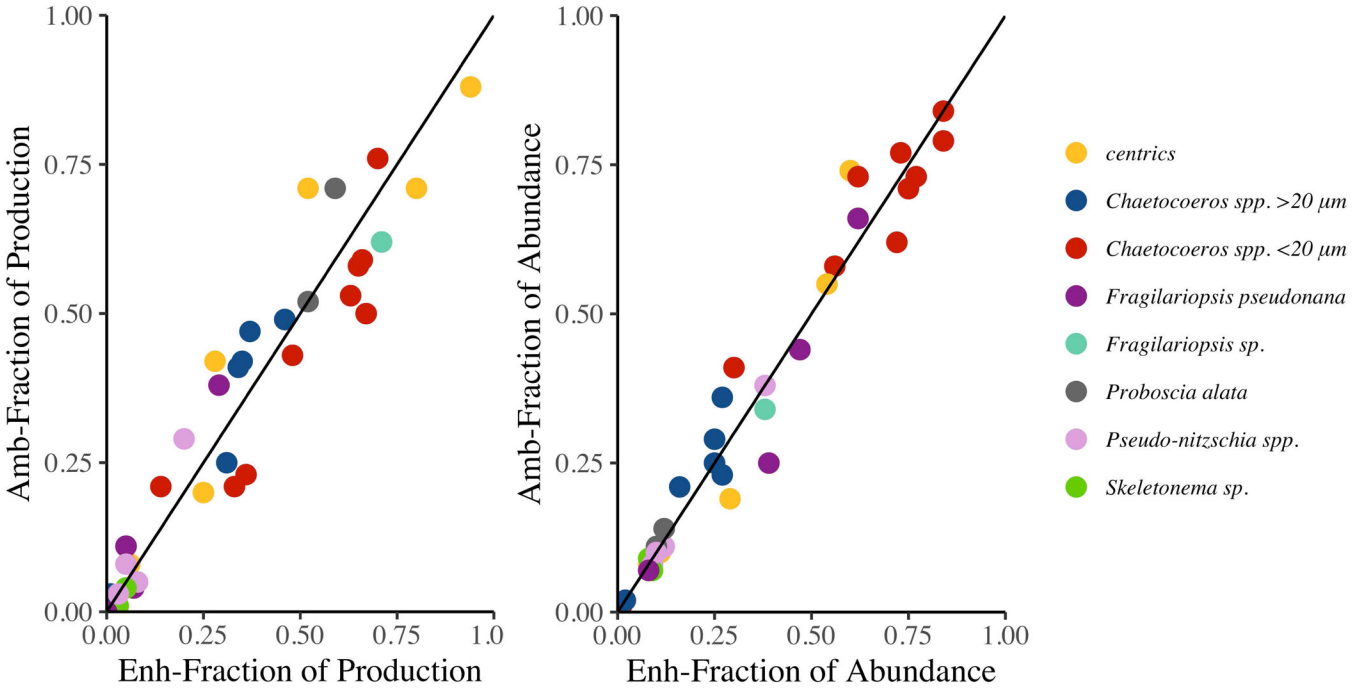

Figure 5:

Changes in fractional production and abundance of taxa in the ambient and +Si treatments. (a) The fractional contribution of taxa to community silica production. (b) The fractional abundance of taxa. In both plots the 1:1 line is depicted as a solid black line.